SAND2015-2632C

Enhanced Infrared Optical Nonlinearities from III-Nitride Heterostructures Coupled to Metamaterials

Omri Wolf[1,2], Andrew A. Allerman[2], Joel Wendt[2], Alex Y. Song[3], Eric A. Shaner[2] and Igal Brener[1,2]

[1]*Center for Integrated Nanotechnologies, Sandia National Laboratories, P.O. Box 5800, Albuquerque, NM, 87185, USA*

[2]*Sandia National Laboratories, P.O. Box 5800, Albuquerque, NM, 87185, USA*

[3]*Electrical engineering department, Princeton University, EQuad, Olden St, Princeton, NJ 08540, USA*

owolf@sandia.gov

Abstract: We demonstrate resonant second harmonic generation from III-Nitride intersubband transitions coupled to metamaterials at wavelengths < 3μm. This approach paves the way for a new class of nonlinear and tunable devices in the near infrared.

OCIS codes: (190.0190) Nonlinear optics; (230.0230) Optical devices; (240.0240) Optics at surfaces

1. Introduction

Parametric processes enable the exploration of quantum phenomena, and the generation of coherent light at new wavelengths where lasing approaches fail. The search for new and highly nonlinear materials is still an active area of research, especially in light of new developments in quantum information science. In the latter context, materials with high second and third nonlinear susceptibilities in the near-infrared are highly desirable, especially because of the availability of single-photon detectors and on-chip processing at those wavelengths.

Large (resonant) nonlinear optical susceptibilities can be obtained from intersubband transitions (ISTs) in semiconductor quantum wells (QWs), by creating equally-spaced quantized electronic levels with good dipolar overlap [1]. Recently, these nonlinearities were enhanced even further by coupling ISTs to metamaterial resonators [2] and nanoantennas [3]. The only way to scale these large optical nonlinearities to the near-infrared is to use semiconductor materials with large conduction band offsets (of the order of several eV). III-Nitride heterostructures naturally provide such offsets.

Here we provide first evidence of very large second order susceptibilities in the short to near IR obtained from ISTs in III-Nitride QWs strongly coupled to metamaterial resonators. Our demonstration was done at λ~3μm but with the proper design and growth, similar results could be obtained in the near-IR. [4**]** The short length of our QW structure coupled to the metasurface (about 1/20th of the free space wavelength) means that we always operate under phase matching conditions. The metamaterial resonators play the dual role of converting the polarization of the pump beam to enable ISTs (electric field must be polarized along the QW growth direction) and increasing the evanescent optical field around the metal traces where the QWs are located [2]. When the metamaterial resonances are properly tuned to the ISTs, this interaction leads to strong coupling [5,6].

2. Sample design and fabrication

Our III-Nitride heterostructures consist of AlN(5nm)/$Al_{0.19}Ga_{0.81}N$(1.4nm)/$Al_{0.8}Ga_{0.2}N$(0.8nm)/$Al_{0.2}Ga_{0.8}N$(1nm) coupled QWs, where the last two layers are nominally n-type doped (Si) to 9x10^{19} cm^{-1} and 5x10^{18} cm^{-1} respectively. 20 periods were grown on previously prepared AlN epilayers on sapphire using MOCVD. Interface sharpness was enhanced by employing a relatively low growth temperature (835 °C) to suppress layer interdiffusion[7].

Fig. 1(a) is a schematic of our finished device consisting of metamaterial resonators coupled to ISTs. Fig. 1(b) shows the measured transmitance of the QW sample measured in a waveguide (wedge) configuration. The two absorption features correspond to the 1>2 and 1>3 transitions and the vertical lines mark the transition energies calculated from the band structure presented in Figure 1(c). This calculation uses an effective

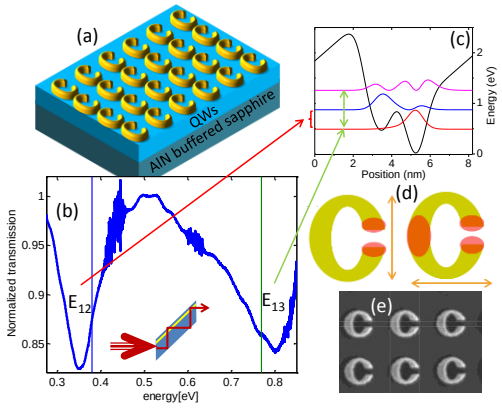

Fig. 1. (a) Schematic of the metamaterial resonators coupled to ISTs for enhanced nonlinearities at short IR wavelengths. (b) Experimental transmission measured in a waveguide (wedge) configuration (bottom inset); the vertical lines denote the calculated values for the marked transitions. (c) Calculated subband energy levels and electron wavefunctions for one period of the QW; the latter were shifted according to their energies. (d) Schematic of the main resonant modes of the SRR (yellow 'C'). The red regions correspond to field 'hot spots' - locations where the out of plane electric field is enhanced. The arrows denote the relevant polarization. (d) SEM micrograph of the fabricated SRR nanocavities on top of the semiconductor sample.

interface grading in order to account for interface roughness known to be present in these heterostructures [8]. Using the calculated wavefunctions and damping coefficients extracted from the measured transmission data we estimate an effective resonant $\chi^{(2)}$ of 1-10 nm/V at energies of 367-383 meV. This $\chi^{(2)}$ is higher than previously reported for single nitride wells[4]. The uncertainty in our calculation arises from experimental ambiguities in the actual dopant activation percentage and the lifetimes of the various levels.

Our metamaterial resonators consist of gold split-ring resonators that were designed to support two resonances as visualized in Fig. 1(d): a *y*-polarized (vertical in the figure) fundamental resonance at ~380 meV; and an *x*-polarized (horizontal in the figure) second harmonic (SH) resonance at ~760 meV. They were patterned on the wafer surface using e-beam lithography, metal evaporation and lift-off. An SEM of the patterned nanocavities is shown in Fig. 1(e). Additional arrays of resonators having resonances detuned from the ISTs were also fabricated on the same die.

3. Measurement setup and results

The device was pumped using a 150 KHz rate OPO laser tuned to the fundamental resonance (3.2um), and the SH signal was measured using a calibrated amplified InGaAs detector. Two control samples were used: (a) an area of the wafer with no metamaterial resonators was measured at Brewster incidence angle (referred below as 'QWs only') and (b) a 250um-thick GaSe crystal oriented for phase-matching conditions. Fig. 2(a) presents the spectral dependence of the measured SH signal as a function of pump photon energy for three cases: i) the red curve corresponds to SH signal from resonators detuned from the ISTs by about 10%, ii) the green curve corresponds to the SH signal when the fundamental resonance of the metamaterial resonators is close to the 1>2 and 2>3 transition energy; iii) the dashed line is the SH signal from the QWs only. This comparison confirms that the enhancement of the SH signal arises from the interaction between the metamaterial resonators and the IST.

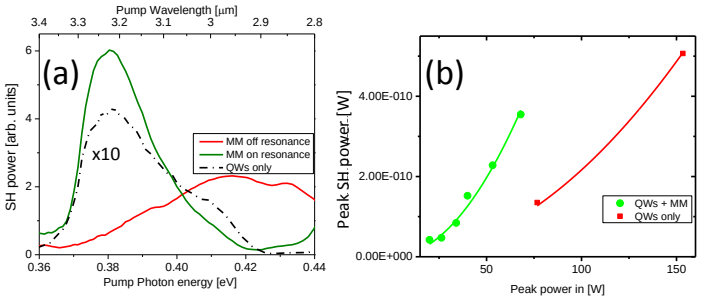

Fig. 2. (a) Spectral dependence of the second harmonic (SH) signals for our device (green line), another device where the MM is 10% detuned from the ISTs (red line) and the QWs alone (dashed line). (b) Peak SH power vs. peak input power for our device and the QWs alone.

Figure 2(b) depicts the SH power as a function of pump power for the device (green) and the QWs alone (red). The lines are quadratic fits where the fitting parameters are found to be $1.7\text{x}10^{-13}$ W/W^2 for our device and $2\text{x}10^{-14}$ W/W^2 for the 'QWs only'. Using previously published theory [9], we derive a $\chi^{(2)}$ for the QWs of ~308 pm/V. This value is higher than previously reported [4], and to verify the various assumptions used in this derivation we used similar measurements from the GaSe crystal and calculated a $\chi^{(2)}$ of 110 pm/V; this is very close to accepted values for GaSe (~112 pm/V [10]). The estimation of the $\chi^{(2)}$ for coupled IST-metamaterial system with III-Nitride materials is not straightforward, but calculations are under way. Similar structures in the mid IR were shown [2,3] to possess effective $\chi^{(2)}$ orders of magnitude higher than bare ISTs.

In an IST system, the theoretical susceptibility is proportional to $\frac{N\mu_{12}\mu_{23}\mu_{13}}{(\omega-\omega_{12}-i\Gamma_{12})(\omega-\omega_{23}-i\Gamma_{23})(\omega-\omega_{23}-i\Gamma_{23})}$, where N is carrier density, μ_{ij}, ω_{ij} and Γ_{ij} are the transition dipole moments, energetic differences and lifetimes respectively between level i and j. Our first results can be improved further by increasing $\chi^{(2)}$ through increases in material quality and uniformity (increase in lifetimes), improvements in electron wavefunction overlaps and perfecting the energetic spacing in this material system. Scaling to shorter wavelengths is potentially possible by growing deeper quantum wells. Furthermore, electrical tuning of the nonlinearities and coupling is also possible [5,9**].**

This work was supported by the U.S. Department of Energy, Office of Basic Energy Sciences, Division of Materials Sciences and Engineering and performed, in part, at the Center for Integrated Nanotechnologies, an Office of Science User Facility operated for the U.S. Department of Energy (DOE) Office of Science. Sandia National Laboratories is a multi-program laboratory managed and operated by Sandia Corporation, a wholly owned subsidiary of Lockheed Martin Corporation, for the U.S. Department of Energy's National Nuclear Security Administration under contract DE-AC04- 94AL85000.

4. References

1. F. Capasso et al. *IEEE J. Quantum Electron* **30**, 1313-1326 (1994).
2. S. Campione et al. *Appl. Phys. Lett.* **104**, 131104 (2014).
3. J. Lee et al. *Nature*. 2014.
4. L. Nevou et al. *Appl. Phys. Lett.* **89**, 151101 (2006).
5. A. Benz et al. *Nat. Comm.***4**, 2882 (2013).
6. S. Campione et al. *Phys. Rev. B* **89**,165133, (2014)
7. J. Wierer et al. *Appl. Phys. Lett.* **97**, 051907 (2010)
8. Y. Song et al. *APS* march meeting 2014
9. C. Sirtori, et al. Appl. Phys. Lett. **59**, pp. 2302-2304, (1991).
10. SNLO nonlinear optics code available from A.V. Smith, AS-Photonics, Albuquerque, NM.